Slab Thinning Controls the Distribution of Large Deep Intraslab Earthquakes in the Western Pacific Subduction Zones

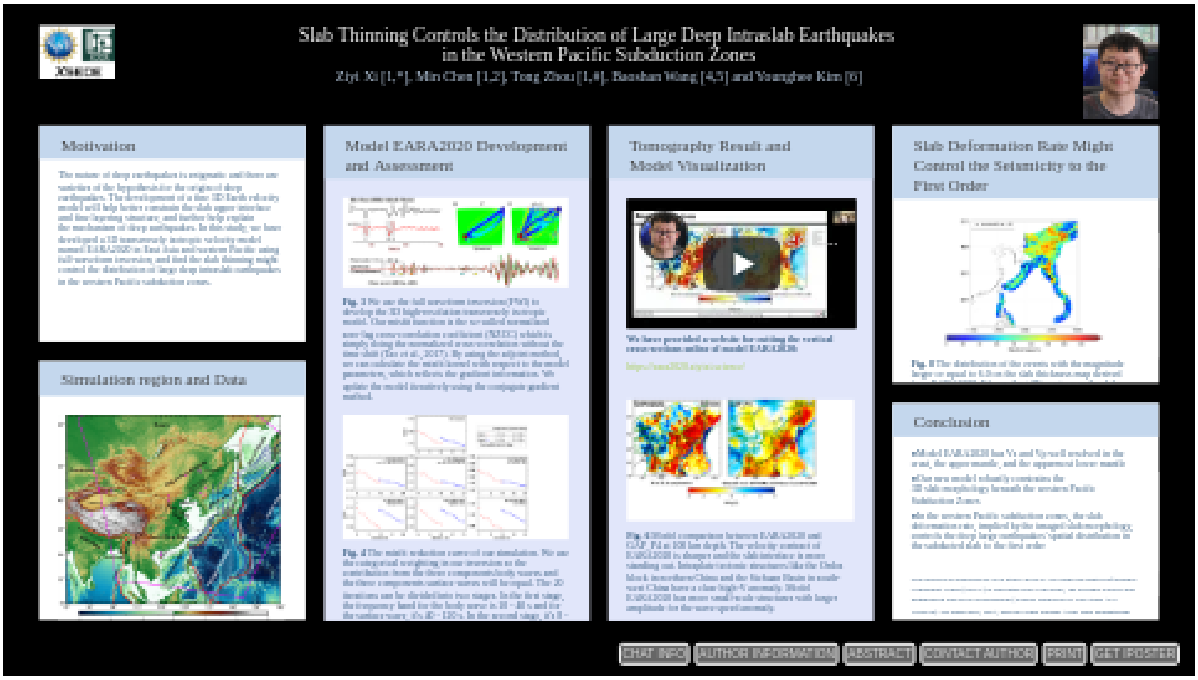

Ziyi Xi [1,*], Min Chen [1,2], Tong Zhou [1,#], Baoshan Wang [4,5] and Younghee Kim [6]

ENTER NAMES OF AFFILIATED INSTITUTIONS

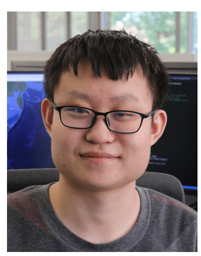

PRESENTED AT:

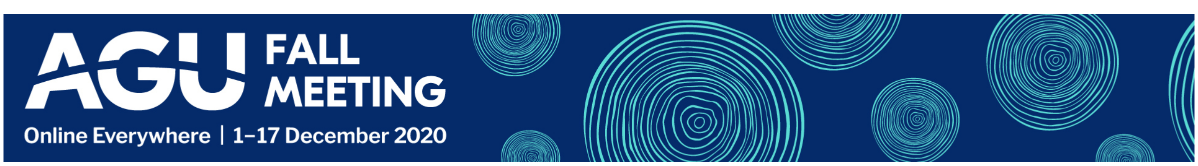

MOTIVATION

The nature of deep earthquakes is enigmatic and there are a variety of hypotheses the hypothesis for the origin of deep earthquakes. The development of a fine 3D Earth velocity model will help better constrain the slab upper interface and fine layering structure, and further help explain the mechanism of deep earthquakes. In this study, we have developed a 3D transversely isotropic velocity model named EARA2020 in East Asia and western Pacific using full-waveform inversion, and find that slab thinning might control the distribution of large deep intraslab earthquakes in the western Pacific subduction zones.

SIMULATION REGION AND DATA

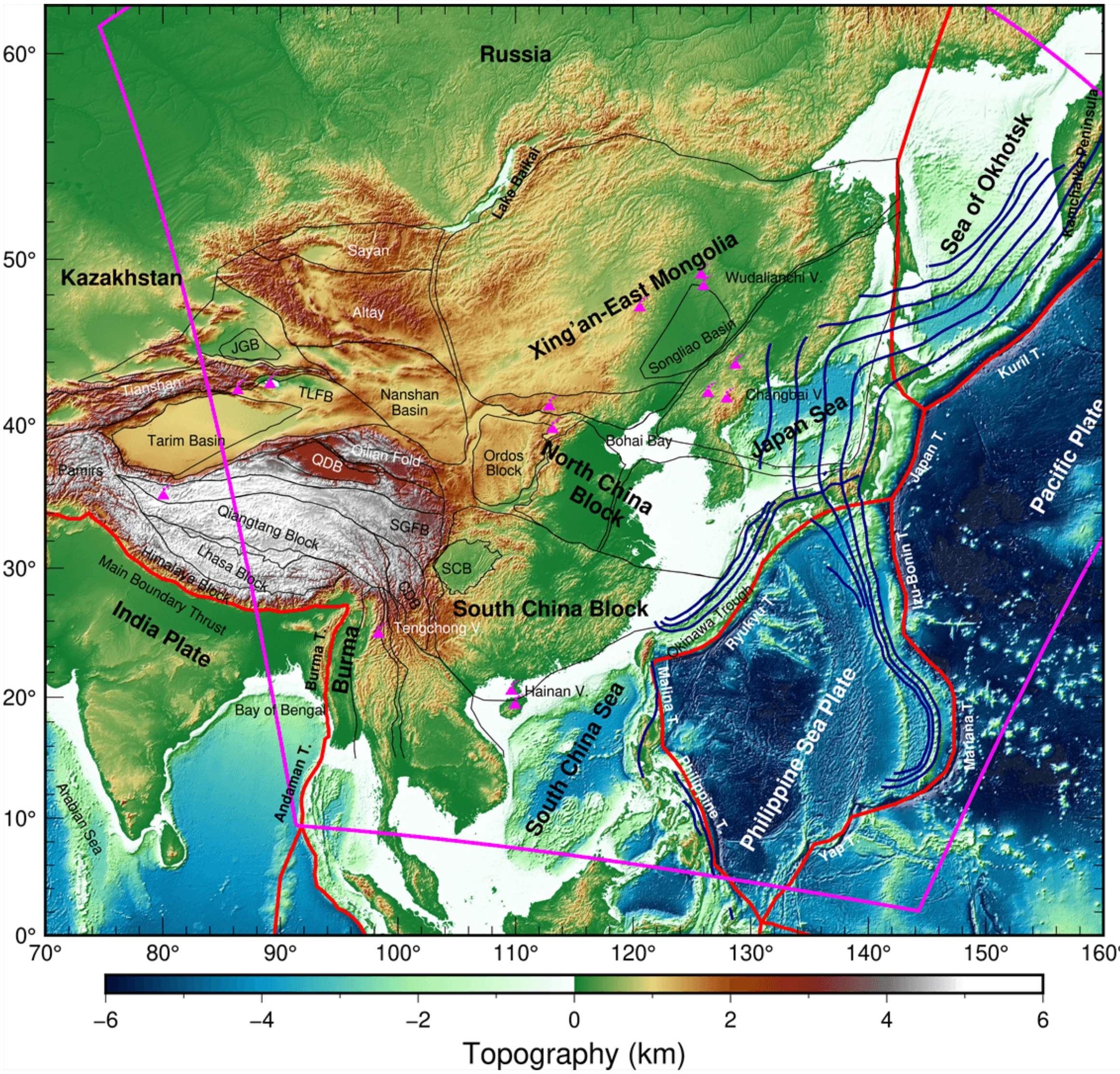

Fig. 1 Tectonic and topographic map of East Asia. The boundary of our simulation region is indicated by the magenta lines. Magenta triangles mark active volcanoes. Blue lines indicate Japan, Kuril and Izu-Bonin slab surface iso-depth from shallow to deep. Dark lines define the main tectonic units and basins. Abbreviations are as follows: CDB, Chuandian Block; JGB, Junggar Basin; QDB, Qaidam Basin; SCB, Sichuan Basin; TLFB, Tulufan Basin; SGFB, Songpan Ganzi Fold Belt. Red bold lines delineate plate boundaries from NUVEL-1 (DeMets et al., 1990).

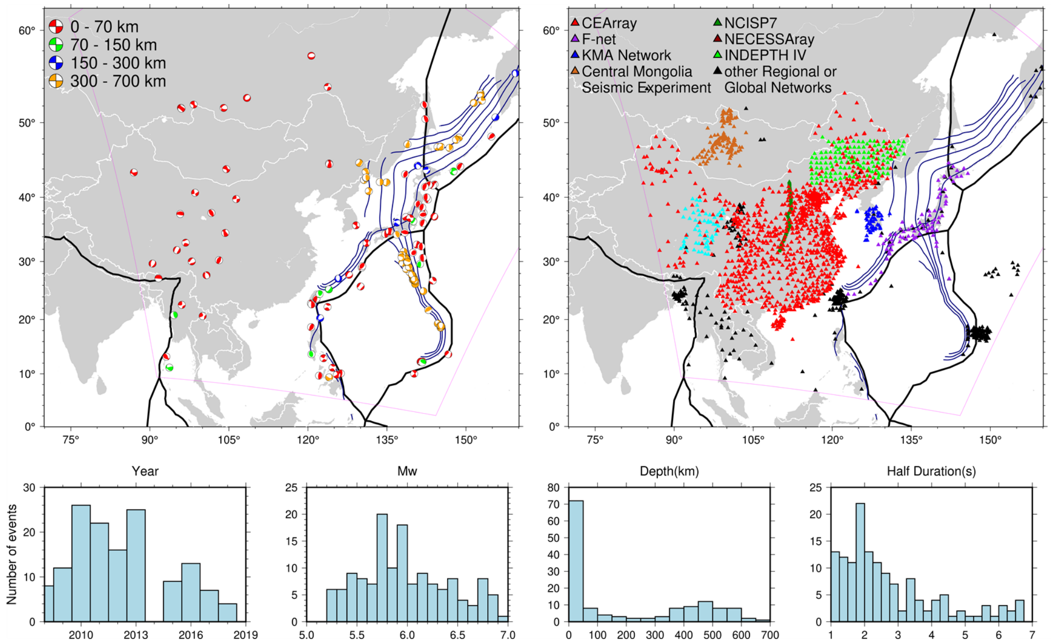

Fig. 2 The events and stations' distribution of our inversion. We select 142 earthquakes from the global centroid moment tensor catalog (Ekström et al., 2012) between 2008 and 2018. These earthquakes are chosen in diverse geographic regions to ensure overall unbiased data coverage in our simulation domain. We also include as many deep events (depth > 150 km) as possible to constrain better the deep mantle structures such as the subducting slabs and the mantle transition zone. The magnitudes (Mw) of the events are chosen between 5.2 and 7 to ensure the minimum influence of finite source complexity and high signal-to-noise-ratio for the waveforms with periods of 8 seconds or longer. We have also further excluded the events with the source half duration greater than 7 s to avoid source complexity that may contaminate the structural inversion. We use three-component waveforms recorded by 2,014 stations from the China Earthquake Administration Array (CEArray) (ZHENG, 2009), F-net (Okada et al., 2004), NECESSAray (Tang et al., 2014), INDEPTH Array (Alsdorf et al., 1998), the central Mongolia seismic experiment (Meltzer et al., 2019), the Korean seismic network and other regional and global seismic networks.

MODEL EARA2020 DEVELOPMENT AND ASSESSMENT

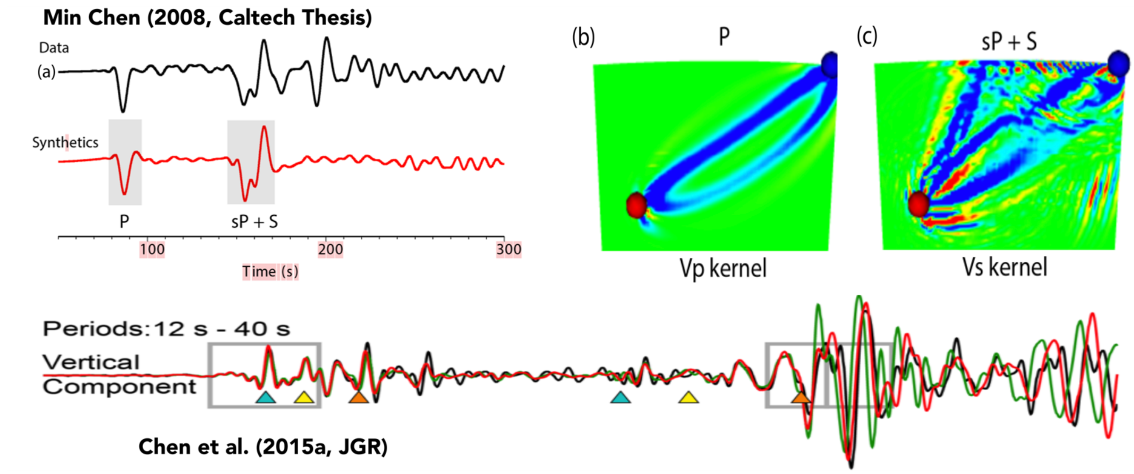

Fig. 3 We use the full waveform inversion (FWI) to develop the 3D high-resolution transversely isotropic model. Our misfit function is the so-called normalized zero-lag cross-correlation coefficient (NZCC) which is simply doing the normalized cross-correlation without the time shift (Tao et al., 2017). By using the adjoint method, we can calculate the misfit kernel with respect to the model parameters, which reflects the gradient information. We update the model iteratively using the conjugate gradient method.

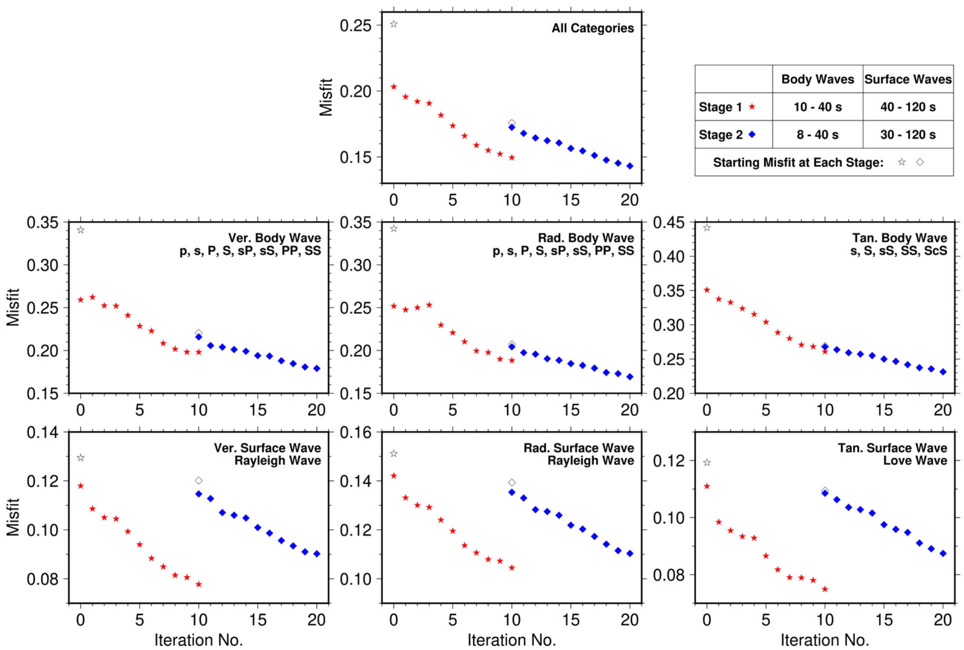

Fig. 4 The misfit reduction curve of our simulation. We use the categorical weighting in our inversion so the contribution from the three components body waves and the three components surface waves will be equal. The 20 iterations can be divided into two stages. In the first stage, the frequency band for the body wave is 10 - 40 s and for the surface wave, it's 40 - 120 s. In the second stage, it's 8 - 40 s for the body wave and 30 -120 s for the surface wave. At the beginning of each stage, we perform the source inversion following the methods in Kim et al., 2011.

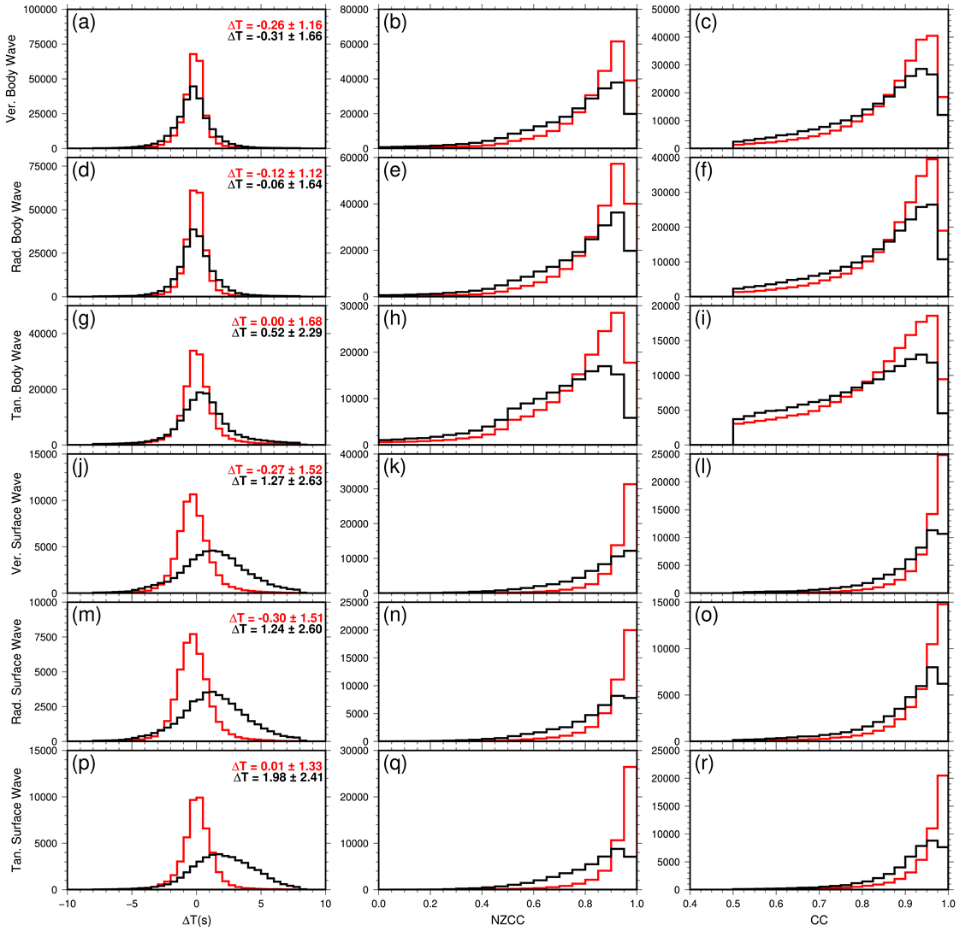

Fig. 5 Comparison between our initial model (black) and final model (red). The first column is for the travel time difference derived from the cross-correlation between the synthetics and the data. The second column is for the NZCC, and the third column is for the cross-correlation coefficient. We can see a significant improvement in the three criteria.

TOMOGRAPHY RESULT AND MODEL VISUALIZATION

[VIDEO] https://www.youtube.com/embed/KFAvghTmiUc?rel=0&fs=1&modestbranding=1&rel=0&showinfo=0

We have provided a website for cutting the vertical cross-sections online of model EARA2020:

https://eara2020.ziyixi.science/ (http://eara2020.ziyixi.science/)

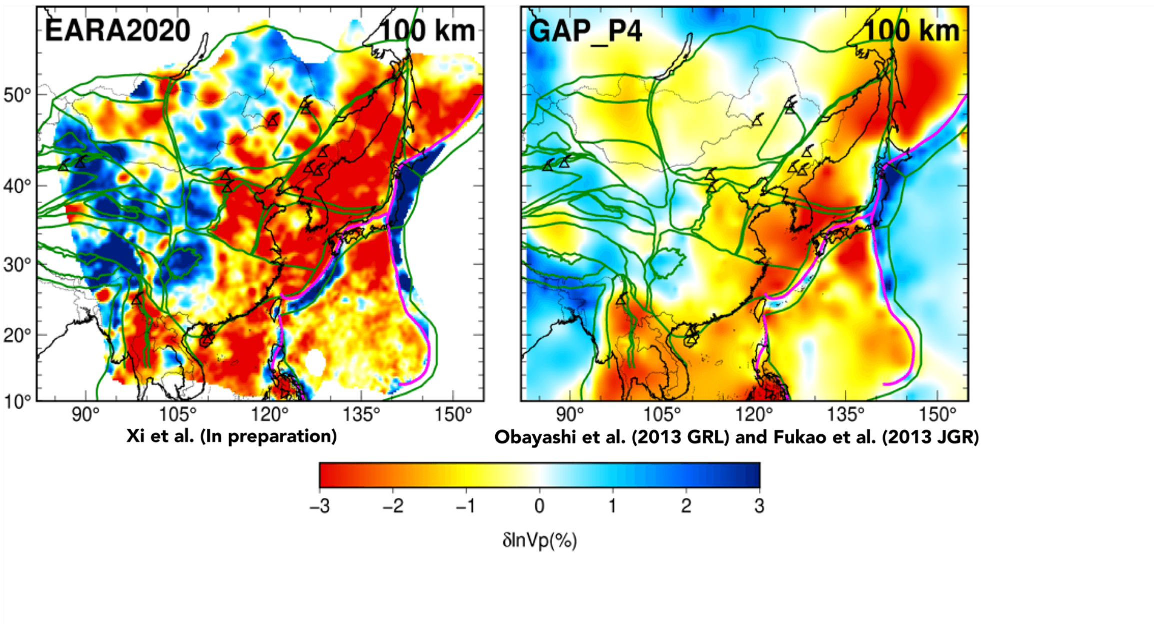

Fig. 6 Model comparison between EARA2020 and GAP_P4 at 100 km depth. The velocity contract of EARA2020 is sharper and the slab interface stands out more. Intraplate tectonic structures like the Ordos block in northern China and the Sichuan Basin in south-west China have a clear high-V anomaly. Model EARA2020 has more small-scale structures with larger amplitude for the wave speed anomaly.

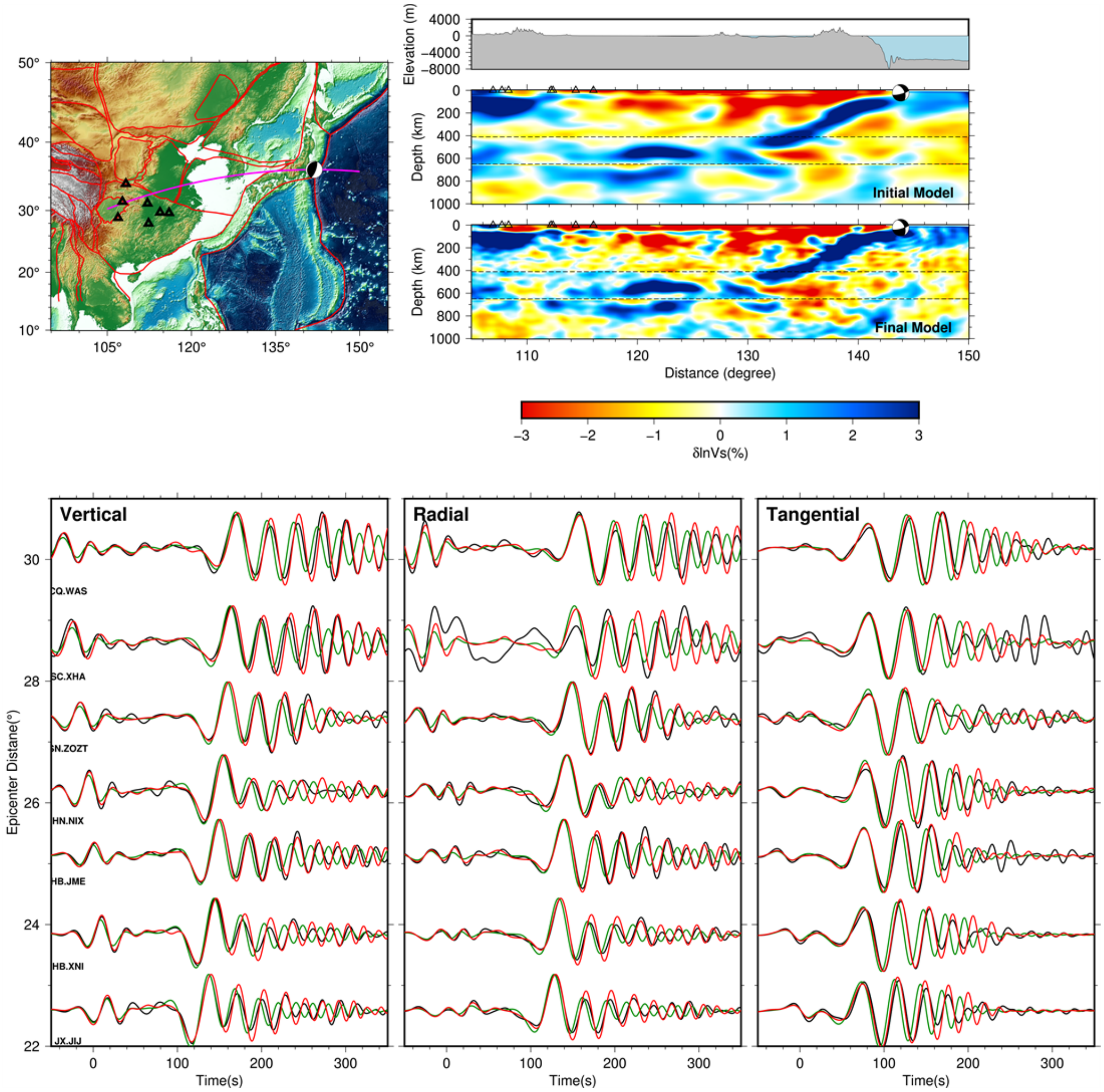

Fig. 7 Three components waveform comparison along the magenta line in the map. The synthetics for EARA2020 (red) fit the data (black) better than the initial model (green). It means the crust and the upper mantle structure of the new model have a significant improvement.

SLAB DEFORMATION RATE MIGHT CONTROL THE SEISMICITY TO THE FIRST ORDER

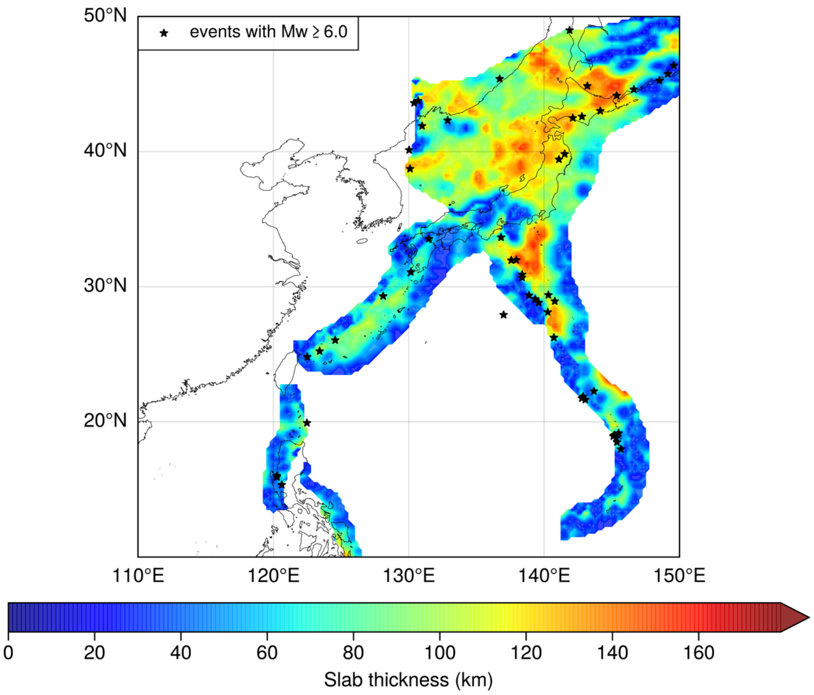

Fig. 8 The distribution of the events with the magnitude larger or equal to 6.0 on the slab thickness map derived from EARA2020. We use the +2% contour as the slab interface. From 25°N to 35°N in the Izu-Bonin slab, the large events' distribution aligns well with the region where the deformation rate for the slab thickness is the largest.

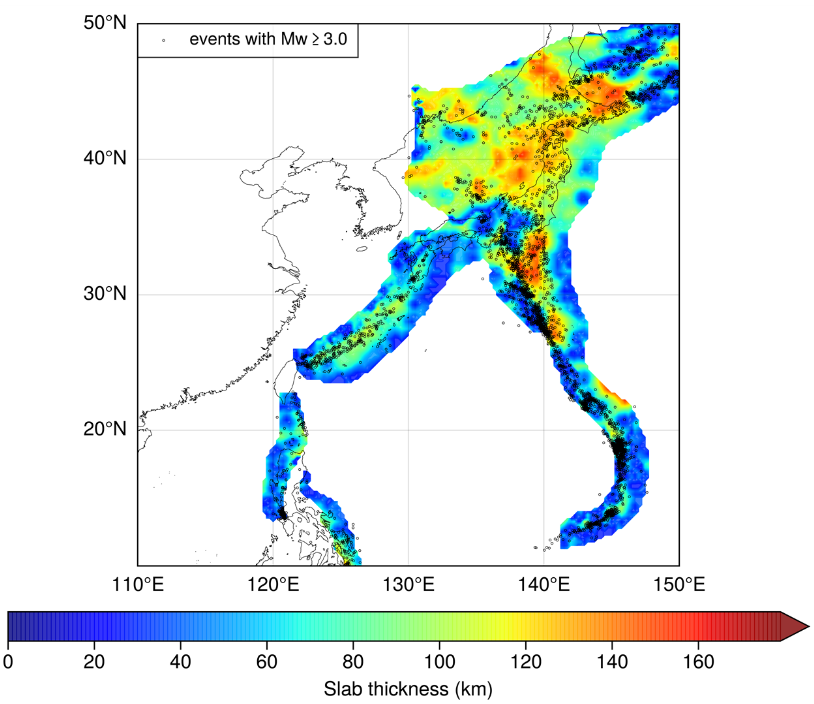

Fig. 9 The same map as above, but for events with the magnitude larger or equal to 3.0. We can see the seismicity distribution from 25°N to 35°N in the Izu-Bonin slab also aligns well with the slab deformation rate.

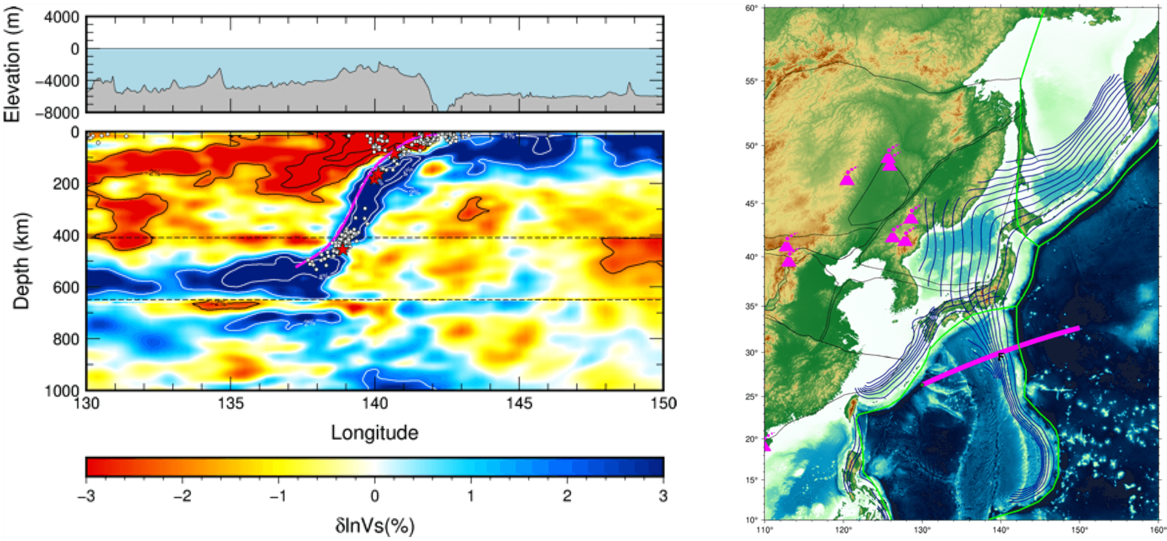

Fig. 10 A vertical cross-section perpendicular to the north Izu-Bonin subduction zone. The slab thins before being stagnant, which is also the region where the earthquakes with the magnitude larger or equal to 3.0 are clustering.

CONCLUSION

●Model EARA2020 has Vs and Vp well resolved in the crust, the upper mantle, and the uppermost lower mantle

●Our new model robustly constrains the 3D slab morphology beneath the western Pacific Subduction Zones

●In the western Pacific subduction zones, the slab deformation rate, implied by the imaged slab morphology, controls the deep large earthquakes' spatial distribution in the subducted slab to the first order

This research is supported by NSF grant 1802247. We thank the High-Performance Computing Center (HPCC) at Michigan State University, the Extreme Science and Engineering Discovery Environment (XSEDE supported by NSF grant ACI-1053575). We thank IRIS, JMA, and the China Seismic Array Data Management Center at the Institute of Geophysics, China Earthquake Administration, for providing the waveform data. We also thank open-source softwares including Obspy, GMT, pygmt, pyasdf and SPECFEM3D Globe. The codes developed for this project has been placed in https://github.com/ziyixi/seisflow (https://github.com/ziyixi/seisflow).

AUTHOR INFORMATION

Ziyi Xi[1,*], Min Chen[1,2], Tong Zhou[1,#], Baoshan Wang[3,4] and Younghee Kim[5]

[1] Department of Computational Mathematics, Science and Engineering, Michigan State University, East Lansing, Michigan 48824, USA

[2] Department of Earth and Environmental Sciences, Michigan State University, East Lansing, Michigan 48824, USA

[3] School of Earth and Space Sciences, University of Science and Technology of China, Hefei, Anhui 230026, China

[4] Institute of Geophysics, China Earthquake Administration, Beijing 100081, China

[5] School of Earth and Environmental Sciences, Seoul National University, Seoul 08826, Korea

[#] Now at University of California Los Angeles, Earth, Planetary, and Space Sciences

[*] Correspondence to: xiziyi@msu.edu

ABSTRACT

The nature of deep earthquakes with depths greater than 70 km is enigmatic because brittle failure at this high-temperature and the high-pressure regime should be inhibited. Three main hypotheses have been proposed to explain what causes deep earthquakes within the subducting slabs, dehydration embrittlement, phase transformational faulting, and thermal runaway instability. However, the existing seismological constraints can’t yet definitively distinguish between these hypotheses because the fine 3D slab structures are not well constrained in terms of slab upper interface, thickness, and internal fine layering. To better image the slabs in the Western Pacific subduction zones, this study employs a full waveform inversion (FWI) that minimizes waveform shape misfit between the synthetics and the observed waveforms from a large dataset, with 142 earthquakes recorded by about 2,400 broadband stations in East Asia. A 3-D initial model that combines two previous FWI models in East Asia (i.e., FWEA18 and EARA2014) are iteratively updated by minimizing the misfit measured from both body waves (8–40 s) and surface waves (30–120 s). Compared to the previous models, the new FWI model (EARA2020) shows much stronger wave speed perturbations within the imaged slabs with respect to the ambient mantle, with maximum perturbation of 8% for Vp and 13% for Vs. Furthermore, the slab thickness derived from EARA2020 exhibits significant downdip and along-strike variations at depths greater than 100 km. The large intra-slab deep earthquakes (Mw>6.0) appear to occur where significant slab thinning happens. This observation suggests that the significant deformation (or strain accumulation) of the slab is likely the first-order factor that controls the distribution of large deep earthquakes within the slab regardless of their triggering mechanism.